Active and passive particles: Modeling beads in a bacterial bath

Guillaume Grégoire,[1] Hugues Chaté,[1] and Yuhai Tu[2]
[1]*CEA, Service de Physique de l'Etat Condensé, Centre d'Etudes de Saclay, 91191, Gif-sur-Yvette, France*
[2]*IBM T.J. Watson Research Center, Yorktown Heights, New York 10598*
(Received 6 October 2000; revised manuscript received 1 January 2001; published 12 June 2001)

A simple model for the motion of passive particles in a bath of active, self-propelled ones is introduced. It is argued that this approach provides the correct framework within which to cast the recent experimental results obtained by Wu and Libchaber [Phys Rev. Lett. **84**, 3017 (2000)] for the diffusive properties of polystyrene beads displaced by bacteria suspended in a two-dimensional fluid film. Our results suggest that superdiffusive behavior should indeed be generically observed in the transition region marking the onset of collective motion.

DOI: 10.1103/PhysRevE.64.011902 PACS number(s): 87.18.Bb, 64.60.Cn, 64.60.Ht

I. INTRODUCTION

Recently, Wu and Libchaber (WL) reported on a fascinating experiment in which bacteria move freely within a two-dimensional fluid film seeded with passive polystyrene beads [1]. They monitored the motion of these beads as an indirect way to study the dynamics of the bacteria as the beads are believed to be pushed around by the bacteria. Indeed, estimating the mean-square displacement of the beads from recorded trajectories, WL found that the average bead velocity is several orders of magnitude larger than thermal fluctuations, confirming the action of bacteria on beads. WL discovered further that fluctuations of the beads' trajectory are not purely diffusive, and that, instead, they follow superdiffusion ($\langle r^2\rangle \sim t^\alpha$ with $1.5<\alpha<2$) below some crossover time and length scales t_c, l_c beyond which normal diffusion ($\alpha=1$) is recovered. They interpret these scales as characteristic of the structures (swirls, jets) that emerge from the collective motion of the bacteria, and use, to fit the experimental data, a Langevin equation for the bead motion with a force term correlated in time over the crossover scale t_c. At a quantitative level, WL found that t_c, l_c, and the asymptotic diffusion constant $D=(1/4)\lim_{t\to\infty} \mathrm{d}\langle r^2\rangle/\mathrm{d}t$ all increase linearly with the bacteria density ρ.

This experiment is characteristic of the general situation in which passive localized tracers are displaced by the motion of active, self-propelled objects—an individual-based version of the passive scalar problem in hydrodynamics (see Ref. [2] and references therein). (Indeed, the collective dynamics of large populations of active ''boids'' [3] was recently shown to be governed by a specific ''hydrodynamic'' equation [4].) Here, we introduce simple models for this general problem, but our main goal remains to obtain a qualitatively faithful, robust, and coherent description of the WL experiment. As a matter of fact, the interpretation proposed by Wu and Libchaber to explain their results suffers from two main problems: first, the Langevin framework predicts ballistic behavior ($\alpha=2$) at short scales, at odds with the nontrivial exponents recorded in the experiment. Second, no attempt is made to explain how or why the typical scales of the collective motion of the bacteria change with their density.

Detailing the conclusions briefly exposed in Ref. [5], we argue below that an appropriate theoretical framework for the WL experiment is that provided by the ''self-propelled *XY* spin'' or boid models studied recently [6,4] complemented by a collection of passive beads. These models allow one to measure simultaneously both boid and bead dynamics. We show first that under very general assumptions, the beads reproduce the diffusive properties of individual bacteria. We then argue that the variation of crossover scales observed by WL corresponds to the onset of long-range orientational order proven recently to exist in minimal models for collective motion. In this framework, crossover scales are expected to diverge at the critical point and true anomalous diffusion at all scales is then observed.

The paper is organized as follows: in Sec. II we recall current knowledge about the basic models for collective motion and introduce one such model adapted to the modeling of the bacterial bath of WL. We also discuss how to implement the motion of passive beads within this model. Section III is devoted to a presentation of the results obtained with our model for the diffusive properties of both active boids and passive beads. Section IV contains conclusions, perspec-

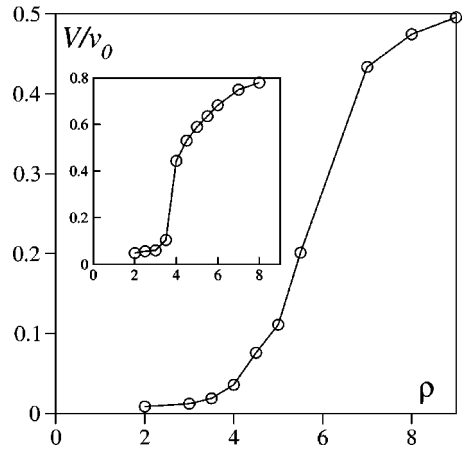

FIG. 1. Variant of Vicsek's core model with repulsive body force between boids, with $v_0=0.3$, $\beta_f=2.5$, $R_b=0.127$, and $\eta=0.5$. Variation of the average velocity amplitude V with boid density ρ in a square domain of linear size $L=128$ with periodic boundary conditions. Inset: same but with noise implemented as in Eq. (4) (system of linear size $L=32$.)

tives, and a general discussion of the relevance of our modeling to the WL experiment.

II. A SIMPLE MODEL

A. Vicsek's core model

The core of the systems studied below is the model introduced by Vicsek *et al.* [6] in which pointwise particles labeled by i (the boids) move synchronously at discrete time steps by a fixed distance v_0 along a direction θ_i. This angle is calculated from the current velocities of all boids j within an interaction range r_0, reflecting the only ''force'' at play, a tendency to align with neighboring boids:

$$\theta_i^{t+1} = \arg\left[\sum_{j\sim i} \vec{v}_j^t\right] + \eta\xi_i^t, \tag{1}$$

where $\vec{v}_i^t$ is the velocity vector of magnitude v_0 along direction θ_i and ξ_i^t is a delta-correlated white noise ($\xi \in [-\pi,\pi]$). Fixing $r_0=1$, the time step $dt=1$ and choosing, without loss of generality, a value $v_0<r_0dt$, Vicsek *et al.* studied the behavior of this simple model in the two-dimensional parameter space formed by the noise strength η and ρ, the boid density. They found, at large ρ and/or small η, the existence of an ordered phase characterized by:

$$V \equiv \langle |\langle \vec{v}_i^t \rangle_i| \rangle_t > 0,$$

i.e., a domain of parameter space in which the boids move collectively. (We used the notation $\langle . \rangle_i$ for the average over all the boids, and $\langle . \rangle_t$ for the average over time.)

This ordered phase was later studied analytically [4] *via* a continuous model for the coarse-grained boid velocity and density. The existence of a broken-symmetry, collective motion state was proven, even in two space dimensions (the case of interest for WL's experiment) and its characteristic scaling exponents were calculated exactly in this last case by renormalization group analysis.

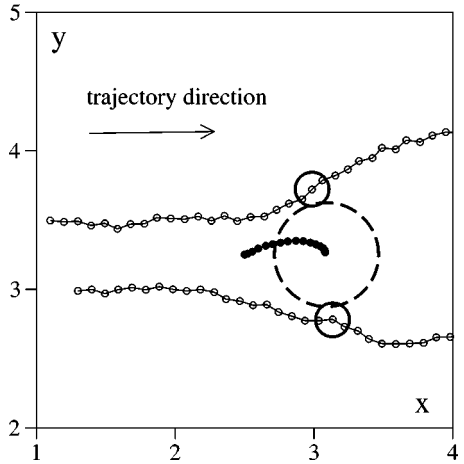

FIG. 2. Two boids setting a bead in motion (interaction rule *A*). The trajectories of two boids coming from the left (open circles) and of the initially immobile bead (filled circles) are represented. Also shown are the actual size of the objects at the time when the boids are about to leave the bead.

TABLE I. Cases of bead-boid interactions considered.

	Reduced mass μ_{Bb}	Entrainment
A	0	yes
B	0.5	yes
C	0.5	no

Vicsek *et al.* devoted most of their effort to studying the transition to the ordered phase [6]. They found numerically a continuous transition characterized by scaling laws and they tried to estimate the corresponding set of critical exponents.

B. A variant

In order to introduce passive beads displaced by the self-propelled boids, we need to give all these objects a finite size (i.e., they cannot be point particles anymore). One of the simplest ways to do so is to add a repulsive body force between boids acting on a typical scale R_b, thus interpreted as the ''radius'' of circular boids. Equation (1) is then replaced by

$$\theta_i^{t+1} = \arg\left[\sum_{j\sim i} (\vec{v}_j^t + \beta_f \vec{f}_{ij})\right] + \eta\xi_i^t, \tag{2}$$

where β_f is a parameter controlling the relative importance of the two ''forces'' and, for example,

$$\vec{f}_{ij} = -\left[1+\exp\left(\frac{r_{ij}}{R_b}-2\right)\right]^{-1}\vec{e}_{ij}, \tag{3}$$

with r_{ij} the distance between boids i and j, and $\vec{e}_{ij}$ the unit vector along the segment going from i to j.

Such a variant of Vicsek's original core model is not expected to show qualitatively different behavior. A first check can be found in Fig. 1, which shows the variation of V as the boid density is increased across ρ^*, the critical value for collective motion.

We have also tested other types of noise terms in the model. In particular, considering the noise as the uncertainty with which each boid ''evaluates'' the force exerted on itself by neighboring boids, leads us to change Eq. (2) to:

$$\theta_i^{t+1} = \arg\left[\sum_{j\sim i} (\vec{v}_j^t + \beta_f \vec{f}_{ij} + \eta\vec{e}_\xi)\right], \tag{4}$$

where $\vec{e}_\xi$ is a unit vector of random orientation. This choice of noise typically makes the transition sharper (the critical region is confined to a rather small window of parameter space) (inset of Fig. 1). We mostly considered, in the follow-

TABLE II. Parameters of the current simulations.

r_0	dt	v_0	R_b	R_B	β_f	β_g	β_h	η	ρ	size
1.0	1.0	0.3	0.127	0.381	2.5	1.0	1.0	0.5	[0;10]	[32;256]

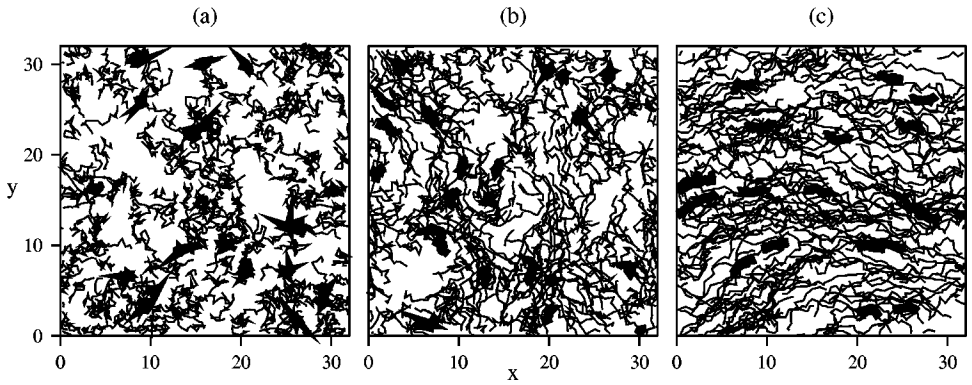

FIG. 3. Short-time trajectories of boids (thin lines) and beads (thick lines) below (a) ($\rho=2.0$), at (b) ($\rho=\rho^*=4.75$), and above (c) ($\rho=8.0$) the critical density ρ^*. In each picture, 230 boid and 20 bead trajectories are shown, during 60 time steps and they were recorded every three steps. System size $L=32, \beta_g=\beta_h=1.0$, bead radius $R_B=0.381$, interaction case *A*, other parameters as in Fig. 1.

ing, the noise term as prescribed in Vicsek's original model, in part because, in the framework proposed below for interpreting WL experiments, the critical region appears to be rather spread out.

C. Passive beads

The beads of WL's experiment can be modeled by circular objects of radius R_B that have no intrinsic velocity nor inertia: they remain immobile when isolated. This is in agreement with the experimental observation by WL that bead's motion is strongly damped by the ambient viscous fluid [1].

The simplest interaction of beads with boids and/or other beads is hard-core repulsion. Such contacts should happen when the current positions of neighboring objects imply an overlap of the circles of radius R_b or R_B characterizing them. A bead of label i with a neighboring object (boid or bead) j of radius R_j such that $r_{ij}<R_B+R_j$ will be displaced from t to $t+1$ by a vector

$$\vec{g}_{ij}=\mu_{ij}[r_{ij}-(R_B+R_j)]\vec{e}_{ij}\,. \tag{5}$$

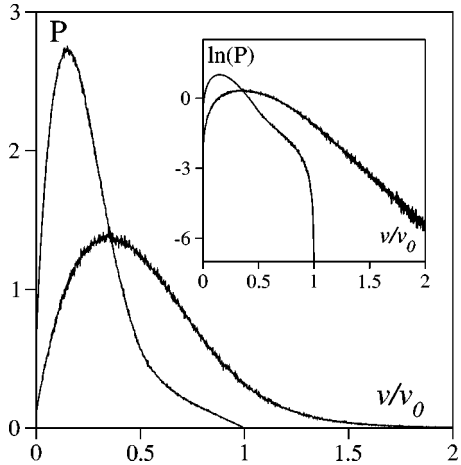

FIG. 4. Probability distribution function of bead velocities. The noisier curve is the PDF of the displacements over three time steps. Inset: logarithm of the same PDF's revealing their exponential tail. Boid density $\rho=2.5$, other parameters as in Fig. 3.

Here, we have introduced ''reduced mass'' μ_{ij}, which controls the relative mobility of the different particles and that takes the value $\mu_{BB}=0.5$ for a collision between two beads, and μ_{Bb} for a collision between a bead and a boid. (For symmetry reasons, a similar displacement will also be exerted on boids by their neighboring beads whenever $r_{ij}<R_b+R_B$, with the corresponding reduced mass $\mu_{bB}=1-\mu_{Bb}$.)

At a coarse-grained level, bead motion is affected by two fluids: the highly viscous, ambient physical fluid and the ''biological fluid'' formed by bacteria. Besides collision, an extra interaction between beads and bacteria can be understood as an ''entrainment'' force exerted on the beads by the local flow of boids. This can be decribed by the ''local bacteria velocity'' felt by bead i. In order to account for the fact that closer boids contribute more to this local velocity, each boid's contribution can be weighted by the bead/boid overlap, leading to following expression for the local bacteria velocity felt by the bead i:

$$\vec{v}_i^{\,\mathrm{loc}}=\frac{1}{\mathcal{N}_i}\sum_{\substack{\text{boids } j\\ r_{ij}<R_B+R_b}}\left(1-\frac{r_{ij}}{R_B+R_b}\right)\vec{v}_j\,, \tag{6}$$

where $\mathcal{N}_i$ is the number of neighboring boids overlapping with the bead i.

The bead motion is driven by the flow of bacteria, but it is also damped by the viscous physical fluid. In the over-

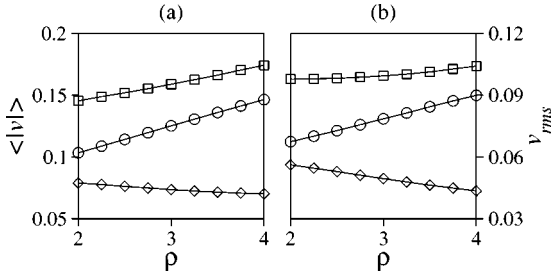

FIG. 5. Mean (a) and rms (b) bead velocity amplitude (not to be confused with the order parameter V!) for case *A* (diamonds), case *B* (squares), and case *C* (circles). Boid density $\rho=2.5$, other parameters as in Fig. 3.

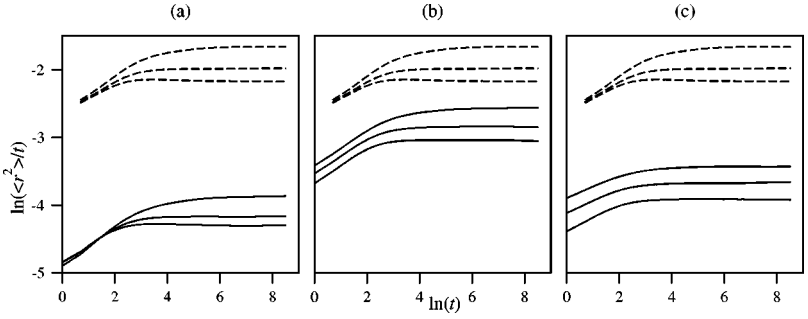

FIG. 6. Typical behavior of $\langle r^2\rangle/t$ vs $\log t$ just below threshold ($\rho=2.0$, 2.50, and 3.0, from bottom up) for boids (dashed lines) and beads (solid lines). (a) interaction case *A*, (b) interaction case *B*, (c) interaction case *C*. Other parameters as in Fig. 3.

damped limit, the velocity of the beads can be simply written as proportional to the weighted local mean velocity $\vec{v}_i^{\,\mathrm{loc}}$:

$$\vec{v}_i^{\,B}=\beta_h\vec{v}_i^{\,\mathrm{loc}}, \tag{7}$$

where, β_h is a constant depending on the fluid viscosity and the strength of the adhesion between bacteria and the beads (or the friction between beads and the bactia flow), which controls the relative importance of hard-core repulsion and entrainment effect.

To summarize:

- A boid i moves over a distance v_0 along the direction:

$$\theta_i^{t+1}=\arg\left[\sum_{\substack{\text{boids } j\\ r_{ij}<r_0}}(\vec{v}_j^{\,t}+\beta_f\vec{f}_{ij})+\sum_{\substack{\text{beads } j\\ r_{ij}<R_b+R_B}}\beta_g\vec{g}_{ij}\right]+\eta\xi_i^t, \tag{8}$$

where β_g controls the relative influence of the collision with beads.

- The position of bead i is updated, in one time step, by its velocity:

$$\vec{v}_i=\sum_{\substack{\text{boids, beads } j\\ r_{ij}<R_B+R_j}}\beta_g\vec{g}_{ij}+\beta_h\vec{v}_i^{\,\mathrm{loc}}. \tag{9}$$

D. Parameters

In this paper, we have chosen, whenever possible, parameter values consistent with those of WL. For those model parameters that can not be extracted directly from the experiment, we have chosen numbers that are reasonable. While further experiments are highly desirable in determining these parameters, at a qualitative level, most of the results we present below are insensitive to the precise choice of these parameters.

Our two main parameters, such as those in Vicsek's core model, are the boid density ρ and the noise strength η. However, following the WL experiment, we vary mostly ρ, keeping η constant. The bead density is always chosen very small (e.g., of the order of 1% of ρ), so that these objects are indeed tracers with no influence on the collective modes of motion. Consequently, beads have a negligible effect on boids [the second sum in Eq. (8)], and bead-bead interactions [in the first sum of Eq. (9)] are rare.

To insure realistic, quasicontinuous trajectories of boids (and beads), the default velocity v_0 has to be substantially smaller than the interaction range r_0 that is set to $r_0=1$ for simplicity. Velocity v_0 cannot, however, be taken too small, for reasons of numerical efficiency. In the following, $v_0=0.3$.

The geometrical parameters R_b, R_B reflect those of the WL experiment: the bacteria are elongated cells roughly $1\times 2-3$ μm, whereas spherical beads of diameter $5-10$ μm

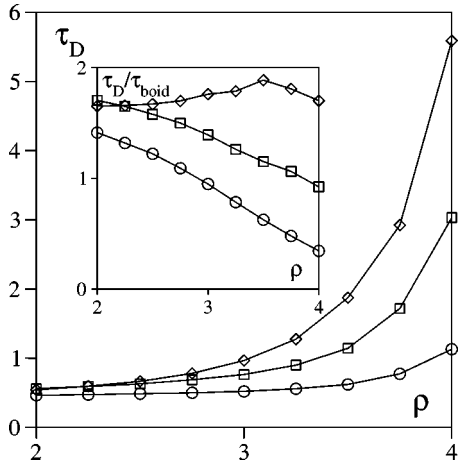

FIG. 7. Comparison of bead effective diffusion time $\tau_D=D_B/v_{rms}^2$ for interaction rule *A* (diamonds), *B* (squares), and *C* (circles). Inset: ratio of the three bead diffusion times over the boid diffusion time $\tau_b=D_b/v_0^2$. Parameters as in Fig. 3.

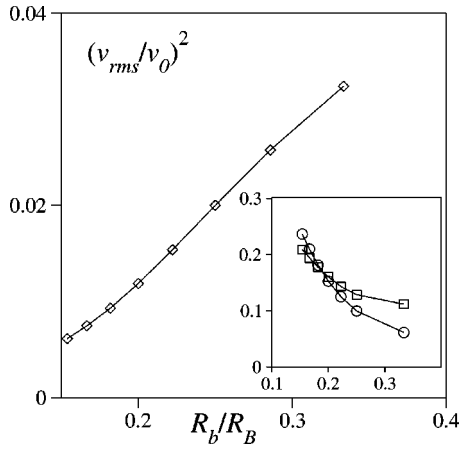

FIG. 8. Bead *rms* velocity (normalized by v_0) vs inverse bead diameter (normalized by boid radius) for interaction case *A*. Inset: same but for case *B* (squares) and case *C* (circles). Boid density $\rho=2.5$, other parameters as in Fig. 3.

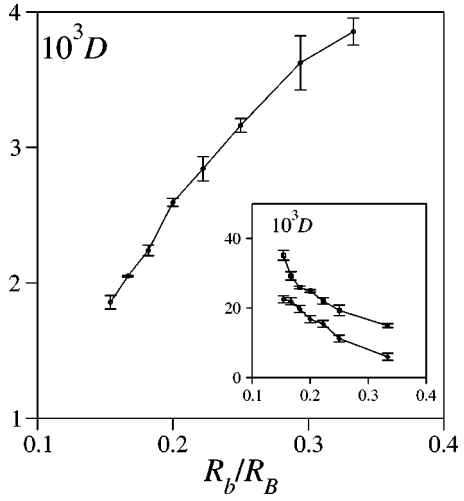

FIG. 9. Same as Fig. 8 but for the bead diffusion constant D_B.

were used. Here, we chose, accordingly, $R_b=0.127$ and $R_B=0.381$.

Below, we present results on three cases corresponding to various interaction rules (Table I). In case *A*, we take $\mu_{Bb}=0$ (in agreement with the mass difference between bacteria and beads in WL's experiment), so that beads are only displaced by the entrainment force. Case *C* is the opposite case, where the entrainment force is set to zero and $\mu_{Bb}=0.5$. Case *B* is intermediate, with both forces present and $\mu_{Bb}=0.5$ also.

Finally, the remaining coefficients tuning the relative importance of the various ''forces'' involved were kept fixed at the following reasonable (order 1) values: $\beta_f=2.5, \beta_g=1.0, \beta_h=1.0$. (For a summary, see Tables I and II)

E. Typical behavior

Figure 2 illustrates how beads are displaced by neighboring boids. In this particular sequence extracted from a typical run, two boids with correlated trajectories encounter an (immobile) bead and set it in motion until they ''flow'' passed it. Clearly, the bead trajectory, at this ''microscopic'' scale, already reflects boids motion.

On a larger scale, Fig. 3 shows short-time trajectories of all boids for three different densities, below, at, and above ρ^*, the critical value for collective boid motion. This representation allows for a clear visualization of the onset of collective motion. In the critical region [Fig. 3(b)], one distinguishes mesoscopic scale structures and large local-density fluctuations. Also represented are the corresponding trajectories of the beads present in this simulation. One can check that they approximately follow the neighboring boid motion.

Whereas the distribution of the amplitude of boid velocities is somewhat meaningless in our model (all boids move with velocity v_0), the distribution of the amplitude of instantaneous bead velocities is nontrivial. It is found to be peaked at a value $\langle|v_B|\rangle$ of the order of v_0. Its tail is roughly exponential — with, of course a finite cutoff scale due to the existence of a maximum possible displacement in one time step (Fig. 4).

The mean and the *rms* values show different behavior for the different interaction cases (Fig. 5). For cases *B* and *C*, these quantities increase with ρ. This is probably due to the fact that the displacement due to collision (present in these two cases since $\mu_{Bb}=0.5$) is additive. At any rate, all cases are consistent with WL measurements of the bead *rms* velocity variations (30%).

III. DIFFUSION PROPERTIES OF BOIDS AND BEADS

We now report on numerical investigations of bead and boid diffusive properties using the simple model described above. We essentially measured the order parameter *V* and the mean-square displacement $\langle r^2\rangle$ as a function of time in the stationary regime following random initial conditions. Below the collective motion onset, we expect the asymptotic behavior of boids to show normal diffusion ($\alpha=1$), whereas ballistic behavior ($\alpha=2$) should be observed in the ordered phase for $\rho>\rho^*$. Around the critical point, intermediate, superdiffusive behavior crossing over to either normal diffusion ($\rho<\rho^*$) or ballistic motion ($\rho>\rho^*$) is observed.

Figure 6 shows typical results just below threshold. A first observation, valid for all cases, is that boids and beads exhibit identical diffusive properties up to a shift in the asymptotic diffusion constant $D=(1/4)\lim_{t\to\infty} d\langle r^2\rangle/dt$. Note that this shift is largely arbitrary since, for beads, D_B depends on the various constants involved in the interaction rules. In fact, the variation of D_B and $\langle|v_B|\rangle$ with ρ or η depends on the interaction rules chosen—in particular, on the relative importance of the mobility during a collision. However, their ratio, i.e., the diffusion time $\tau_D \equiv D_B/\langle|v_B|\rangle^2$ remains roughly of the same order of magnitude (Fig. 7), irre-

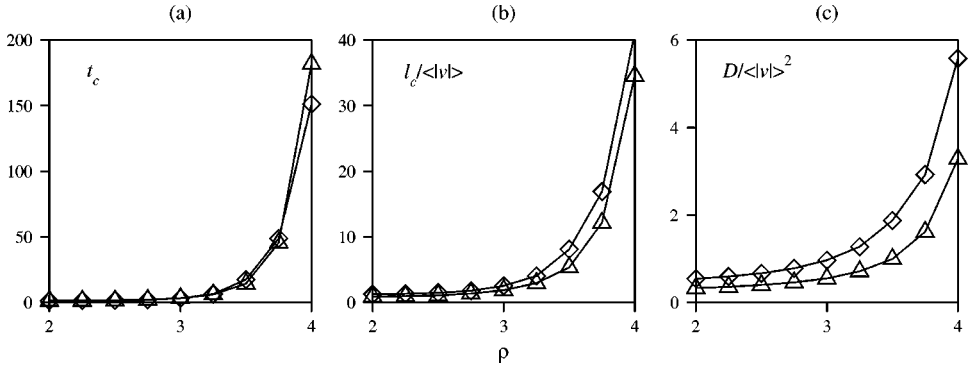

FIG. 10. Comparison of bead (diamonds) and boid (triangles) crossover quantities for interaction rule *A* as the boid density ρ is varied.

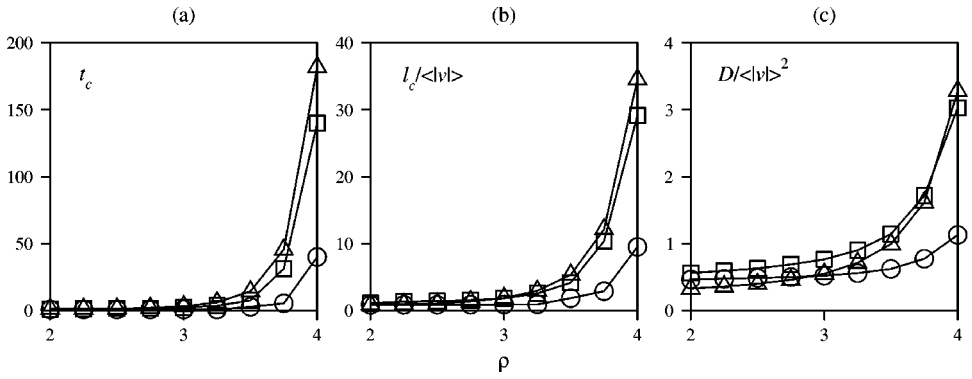

FIG. 11. Same as Fig. 10 but for interaction rules *B* (squares) and *C* (circles).

spective of the bead-boid interaction rule chosen. However, the three curves diverge from one to another when approaching the critical point. Case *A* is the bead/boid interaction choice that makes boid and bead diffusive behavior most similar (inset of Fig. 7), but, anyway, all cases reveal the divergence of the diffusion constant near the critical point.

A. Influence of bead radius

Wu and Libchaber report on experiments done with beads of two different diameters, and they observed that the bead diffusion constant D decreases with increasing R_B, in a manner compatible with the Stokes-Einstein relation, i.e., $D \propto 1/R$. Here, our model allows us to check in more detail whether this relation holds. Figures 8 and 9 show that both the diffusion constant D and the rms velocity do vary like $1/R$ for the interaction rule *A*. This confirms the relevance of a Stokes-Einstein-like law and gives more weight to the remark made by WL about the lack of equipartition of energy probably due to the role of hydrodynamic interactions [1]. However, for cases *B* and *C*, the above relationships are *not* verified, suggesting further that the ''best'' modeling choice, i.e., the most consistent with WL's experiment, is the interaction rule *A* (insets of Figs. 8 and 9).

B. Defining crossover scales

Keeping the bead radius R_B constant, we now report on the behavior of our model when ρ, the density of boids, approaches the critical value ρ^*. In order to quantify the variation of crossover scales seen in Fig. 6, the ansatz proposed by WL in their Langevin dynamics approach cannot be used since it cannot account for a true superdiffusive behavior, but only for a crossover from ballistic to diffusive motion.

Thus, we introduce the following *ad hoc* ansatz for the mean-square displacement of both boids and beads:

$$\langle r^2 \rangle(t) \simeq \frac{4Dt}{(t/t_c)^{1-\alpha}+1}. \qquad (10)$$

This equation does interpolate between a superdiffusive behavior ($\alpha > 1$) at short times and a standard diffusive behavior at long times, the crossover time t_c being explicitly defined. All our data is very well fitted with Eq. (10).

A crossover length scale l_c can then be defined as the mean displacement at time t_c. Using Eq. (10), one has

$$l_c^2 = 2Dt_c.$$

The recorded crossover time t_c is identical for boids and beads [Figs. 10(a) and 11(a)] whereas the crossover length and diffusion constant are different but vary similarly. In fact, the observed difference in the crossover length l_c disappears once l_c is normalized by the mean velocity (i.e., v_0 for boids and $\langle |v| \rangle$ for beads) [Figs. 10(b) and 11(b)]. Similarly, normalizing D by $\langle |v| \rangle^2$, yields diffusion constants of the same order of magnitude for boids and beads [Figs. 10(c) and 11(c)].

C. Discussion

In their experiment, WL found that the crossover scales of the bead diffusive properties vary roughly linearly with the bacteria density. Within the framework of our model (and all Vicsek-like models), however, the crossover scales of both

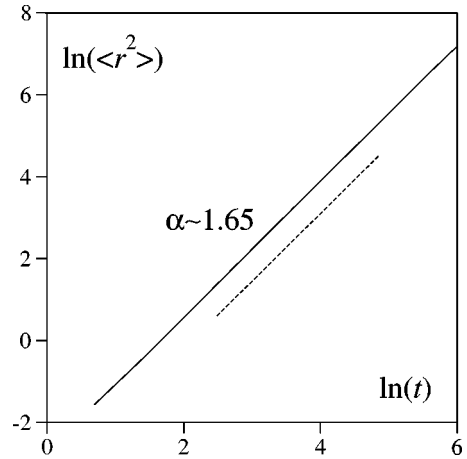

FIG. 12. Pure superdiffusive behavior at threshold as recorded from the mean-square displacement of boids. $L_x = L_y = 256$, $\rho = 2$, $\eta^* = 0.385$, $\beta_f = 2.5$, $R_b = 0.127$. A transient of 2^{17} time steps was observed before averaging during 45 loops of 3000 time steps for 1024 boids. The critical noise strength η^* was given by the preliminary results of an ongoing finite-size scaling analysis. A fit by a power law yields an exponent $\alpha \simeq 1.65(5)$. The precise value of α in the asymptotic limit as well as its universality are currently under investigation [7].

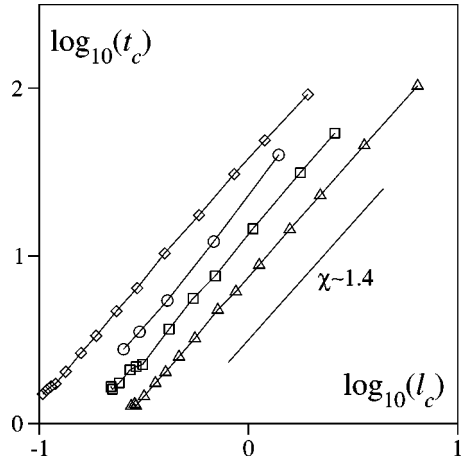

FIG. 13. Log-log plot of the crossover time as a function of the crossover length for boids (triangles) and beads with interaction rules *A* (diamonds), *B* (squares), and *C* (circles).

boid and bead behavior all diverge when approaching the critical boid density ρ^*, leaving pure superdiffusive behavior at threshold (Fig. 12).

We believe this discrepancy is only due to the fact that WL effectively probed a domain of variation of bacteria density rather far from the critical point. Indeed, the maximal value of l_c they report is of the order of the size of their beads. Our data for the crossover scales, when limited to such a range, can actually also be fitted rather well by a linear dependence.

Similarly, WL's observation that the rms velocity of beads is independent of the bacteria density and their subsequent linking of this to the observed proportionality of l_c and t_c presumably only hold in the restricted off-critical range of densities they scanned. The data provided by our model rather reveal, consistently with the idea of a critical point at $\rho=\rho^*$, an algebraic relationship between t_c and l_c in the critical region (Fig. 12). Indeed, as Fig. 13 shows, we observe $t_c \sim l_c^{\chi}$ with $\chi \simeq 1.4$ for boids and beads, whatever the interaction rule chosen.

IV. CONCLUSION AND PERSPECTIVES

We have introduced a simple model for the motion of passive beads in a noisy bath of active ''boids'' interacting only locally. While our primary aim was to perform an analysis similar to that of the WL experiment, our approach is rather general and our results very robust. At a qualitative level, they are largely independent of the choice of parameters, precise form of interaction forces, etc. Our approach also shows explicitly that the origin of the crossover scales observed by WL from the bead motion are identical to the typical scales of the collective motion of bacteria/boids.

The robustness of our model's properties and the overall good agreement between our observations and those of WL make us confident that the framework put forward here is the relevant one to describe experiments of that kind. In particular, our conclusions indicate that true superdiffusive motion (and not simple ballistic motion) of both bacteria and passive bead tracers is present, and that this should become more easily observable experimentally as the density of bacteria is increased. New experiments in this direction are thus desirable, since the observation of superdiffusive behavior over a large range of scales would definitely rule out the possibility of a simple crossover from a short-scale behavior (due to individual bacterium motion) to normal diffusion.

At a quantitative level, no precise agreement can be expected from the approach taken here. Indeed, many of the bacteria bath properties are still unknown, and their precise translation into features of models such as ours remains impossible [8]. However, the vicinity of the (expected) threshold of long-range collective motion should allow for quantitative comparison. Indeed, in the spirit of critical phenomena studies, the scaling laws attached to the critical point are expected to be universal. In this respect, an experimental evaluation of the exponent α and its comparison with its value as determined from analytical or numerical studies would be most interesting. Ongoing work aims at the determination of reliable estimates for the set of critical exponents characterizing the transition to collective motion [7].

[1] X. -L. Wu and A. Libchaber, Phys. Rev. Lett. **84**, 3017 (2000).
[2] B.I. Shraiman and E.D. Siggia, Nature (London) **405**, 639 (2000).
[3] ''Boid'' is the contraction of ''bird-oid,'' a term used in animation graphics. See, e.g., C. Reynolds, Comput. Graph. **25**, 21 (1987).
[4] J. Toner and Y. Tu, Phys. Rev. Lett. **75**, 4326 (1995); Phys. Rev. E **58**, 4828 (1998).
[5] G. Grégoire, H. Chaté, and Y. Tu, Phys. Rev. Lett. **86**, 556 (2001).
[6] T. Vicsek, A. Czirók, E. Ben-Jacob, I. Cohen, and O. Shochet, Phys. Rev. Lett. **75**, 1226 (1995); A. Czirók, H.E. Stanley, and T. Vicsek, J. Phys. A **30**, 1375 (1997).
[7] G. Grégoire, H. Chaté, and Y. Tu (unpublished).
[8] X.-L. Wu and A. Libchaber, Phys. Rev. Lett. **86**, 557 (2001).